DOI: 10.24412/2181-144X-2026-2-5-13 Sayfidinova M., Khaydarov O., Mardonov B.

COMPARATIVE INVESTIGATION OF HADFIELD STEEL BY SEM–EDS AND ITS STEELMAKING SLAG BY LIBS: MICROSTRUCTURAL AND CHEMICAL CORRELATIONS

Sayfidinova M., [1][0009-0004-2355-1494], ***Khaydarov.O.,*** [2][0009-0000-7157-0156], ***Mardonov B.*** [3][0009-0007-9553-263]]

[1]PhD student at the Mechanical Engineering Department, Navoi State University of Mining and Technologies, E-mail: sayfidinova.mk@gmail.com
[2]Master student at the Mechanical Engineering Department, E-mail: oybekkhaydaroff@gmail.com
[3]Professor at Mechanical Engineering Department, E-mail: mbt69@mail.ru

Abstract. Hadfield (high-manganese austenitic) steel and the slag generated during its production were investigated using two complementary analytical techniques: scanning electron microscopy with energy-dispersive X-ray spectroscopy (SEM–EDS) for the solid steel, and laser-induced breakdown spectroscopy (LIBS) together with optical three-dimensional profilometry for the steelmaking slag. The steel, produced in an electric arc furnace at the Navoi Machine Building Plant, exhibited an iron-rich austenitic matrix with manganese as the principal alloying element, together with carbon, oxygen and silicon. Spatially resolved line scans and elemental maps revealed a localised oxygen- and carbon-enriched, iron- and manganese-depleted region, which was identified as a (Fe,Mn)-oxide–silicate non-metallic inclusion. LIBS analysis of the associated slag identified a calcium-, silicon- and potassium-bearing calcium compound, while three-dimensional profilometry measured a surface relief of up to 44.86 µm. These two data sets are closely correlated: the oxide-silicate inclusions trapped in the steel belong to the same chemical class as the bulk slag, indicating that these inclusions are essentially microscopic slag particles trapped within the metal. The study demonstrates that combining microscale SEM-EDS with fast volumetric LIBS provides a consistent description of the steel-slag system from the microscale to the bulk, which has direct implications for steel cleanliness, manganese recovery, and the reuse of calcium-rich slag in building materials.

Key words: Hadfield steel, high-manganese austenitic steel, SEM–EDS, LIBS, steelmaking slag, non-metallic inclusions, surface profilometry.

Annotatsiya. Hadfild (yuqori marganesli austenit) po‘lati va uni ishlab chiqarish jarayonida hosil bo‘lgan shlak ikki bir-birini to‘ldiruvchi tahlil usuli yordamida o‘rganildi: qattiq po‘lat uchun energiya dispersion rentgen spektroskopiyasi bilan jihozlangan skanerlovchi elektron mikroskopiya (SEM–EDS), po‘lat eritish shlaki uchun esa lazer yordamida hosil qilinadigan parchalanish spektroskopiyasi (LIBS) va optik uch o‘lchovli profilometriya. Navoiy mashinasozlik zavodida elektr yoyli pechda ishlab chiqarilgan po‘lat temirga boy austenit asosga ega bo‘lib, asosiy legirlovchi element sifatida marganes, shuningdek uglerod, kislorod va kremniyni o‘z ichiga oladi. Fazoviy aniqlikdagi chiziqli skanerlash va elementlar xaritalari kislorod hamda uglerodga boyigan, temir va marganesga kambag‘al mahalliy sohani aniqladi; bu soha (Fe,Mn)-oksid–silikat metall bo‘lmagan qo‘shilma sifatida tavsiflandi. Tegishli shlakni LIBS bilan tahlil qilish kalsiy, kremniy va kaliy saqlovchi kalsiy birikmasini aniqladi, uch o‘lchovli profilometriya esa 44,86 µm gacha bo‘lgan sirt relyefini o‘lchadi. Ikkala ma’lumotlar to‘plami bir-biri bilan chambarchas bog‘liq: po‘lat ichida tutilib qolgan oksid–silikat qo‘shilma asosiy shlak bilan bir xil kimyoviy oilaga mansub bo‘lib, qo‘shilmalar mohiyatan metallda saqlanib qolgan mikro-miqyosdagi shlak ekanligini ko‘rsatadi. Tadqiqot mikro-miqyosdagi SEM–EDS ni tezkor ko‘lamli LIBS bilan birlashtirish po‘lat–shlak tizimining mikrodan makro miqyosgacha yaxlit tavsifini berishini va bu po‘lat tozaligi, marganesni qayta tiklash hamda kalsiyga boy shlakni qurilish materiallarida qayta ishlatish uchun ahamiyatga ega ekanligini ko‘rsatadi.

Kalit so‘zlar: Hadfild po‘lati, yuqori marganesli austenit po‘lat, SEM–EDS, LIBS, po‘lat eritish shlaki, metall bo‘lmagan qo‘shilmalar, sirt profilometriyasi.

Аннотация. Сталь Хадфилда (высокомарганцевая аустенитная) и шлак, образующийся при её производстве, были исследованы с помощью двух взаимодополняющих аналитических методов: сканирующей электронной микроскопии с энергодисперсионной рентгеновской спектроскопией (SEM–EDS) для твердой стали и лазерной спектроскопии с индуцированным разрядом (LIBS) в сочетании с оптической трехмерной профилометрией для сталеплавильного шлака. Сталь, произведенная в

электродуговой печи на Навоиском машиностроительном заводе, имела богатую железом аустенитную матрицу с марганцем в качестве основного легирующего элемента, а также углеродом, кислородом и кремнием. Линейные сканирования с пространственным разрешением и элементные карты выявили локализованную область, обогащенную кислородом и углеродом и обедненную железом и марганцем, которая была идентифицирована как неметаллическое включение из (Fe,Mn)-оксида-силиката. Анализ LIBS соответствующего шлака выявил соединение кальция, содержащее кальций, кремний и калий, в то время как трехмерная профилометрия зафиксировала рельеф поверхности до 44,86 мкм. Эти два набора данных тесно взаимосвязаны: оксидно-силикатные включения, удерживаемые в стали, относятся к тому же химическому классу, что и основная масса шлака, что указывает на то, что эти включения представляют собой, по сути, микроскопические частицы шлака, удерживаемые внутри металла. Исследование демонстрирует, что сочетание микромасштабного SEM-EDS с быстрым объемным LIBS обеспечивает согласованное описание системы «сталь-шлак» от микромасштаба до объемного уровня, что имеет прямое отношение к чистоте стали, извлечению марганца и повторному использованию богатого кальцием шлака в строительных материалах.

Ключевые слова: сталь Гадфильда, высокомарганцевая аустенитная сталь, SEM–EDS, LIBS, сталеплавильный шлак, неметаллические включения, профилометрия поверхности.

Introduction

High-manganese austenitic steel, traditionally known as Hadfield steel, typically contains between 11 and 14% by weight of manganese and 1.0 to 1.4% by weight of carbon. These elements stabilise the austenitic structure at room temperature and give the steel an exceptional combination of toughness, ductility and work hardening [1], [2]. Under the effects of impact and abrasion, the austenite hardens rapidly whilst the core of the steel retains its toughness. This is why, more than a century after its introduction, this steel remains the material of choice for crusher jaws, level crossings, excavator teeth and grinders [3], [4]. The alloy is most commonly melted in electric arc or induction furnaces from scrap and ferromanganese, and its final microstructure and properties are strongly governed by melting temperature, deoxidation practice and the resulting non-metallic inclusions [5], [6].

Steelmaking slag is the principal by-product of these processes. It is a multi-component oxide system dominated by calcium oxide (CaO) and silica (SiO_2), with iron oxides (FeO, Fe_2O_3) and minor manganese oxide (MnO), magnesium oxide (MgO) and alumina (Al_2O_3); its exact composition varies with furnace type, steel grade and refining practice [7], [8]. Thanks to this oxide chemistry, slag is increasingly being put to good use rather than discarded: as aggregate in concrete and road foundations, as a supplementary cementitious material, as a soil improver, and as a low-cost adsorbent for water treatment – all of which contribute to the steel industry's circular economy objectives. [9], [10], [13]. The same chemistry, however, also makes slag chemically heterogeneous and raises concerns over the leaching of metals, so reliable chemical characterisation is essential before reuse [11], [12].

Crucially, the steel and its slag are not independent materials but two products of the same refining chemistry. Strong deoxidisers such as manganese and silicon react with dissolved oxygen to form oxide products that either float out into the slag or remain trapped in the metal as non-metallic inclusions [17]. The micro-scale inclusions inside the steel and the bulk slag therefore originate from a common oxide-forming process. Characterising both sides of this balance calls for complementary tools: scanning electron microscopy with energy-dispersive X-ray spectroscopy (SEM–EDS) resolves the morphology and chemistry of individual inclusions and the steel matrix, whereas laser-induced breakdown spectroscopy (LIBS) provides rapid, near-line, multi-element analysis of slag, including light elements, and has been demonstrated for routine slag monitoring at operating steel works [15, 16].

This study applies both techniques to a single Hadfield steel heat produced at the Navoi Machine Building Plant: SEM–EDS to the solid steel and LIBS, together with optical three-dimensional profilometry, to the corresponding slag. There are several objective such

as (i) to characterise the microstructure and elemental composition of the steel, (ii) to determine the surface morphology and chemistry of its slag, and (iii) to establish the chemical correlation between the non-metallic inclusions retained in the steel and the slag, linking the micrometric and macroscopic descriptions of the steel-slag system.

Materials and Methods

Investigated steel was a high-manganese austenitic steel (Hadfield) grade 110G13L (110Г13Л) smelted in an electric arc furnace at the Navoi Machine-Building Plant from steel scrap and ferromanganese. From a cast piece a solid sample was taken for microstructural analysis, embedded, ground and mirror-polished. The slag formed in the same smelting process was collected and a representative solidified fragment was prepared for surface examination and chemical analysis. Thus both products are obtained from the same refining process so that a direct comparison between the steel and the slag.

SEM–EDS analysis of the steel.

The polished steel sample was examined by scanning electron microscopy (SEM) using an Oxford Instruments energy-dispersive X-ray (EDS) spectrometer controlled by AZtec software and quantified by Tru-Q. Imaging and analysis were done at an acceleration voltage of 15.00 kV and a working distance of 9.59 mm, for a nominal magnification of 500×. Three EDS modes were used in combination: surface and spot spectra to obtain the overall elemental signature; a linear scan across a representative microstructure to map the compositional variation along a profile; and X-ray elemental mapping to visualise the two-dimensional distribution of individual elements. The elements analysed were carbon, oxygen, silicon, chlorine, chromium, manganese, iron, copper, phosphorus and sulphur. The EDS results were obtained without using a standard and normalised and minor signals related to the surface were interpreted with caution because they could be artefacts related to sample preparation rather than constituents of the volume [19].

LIBS and surface profilometry of the slag.

The slag fragment was analysed using a KEYENCE EA-300 series element-analysis system based on laser-induced breakdown spectroscopy. In LIBS, a focused pulsed laser ablates a microscopic volume of the sample and generates a plasma whose optical emission is spectrally resolved to identify and semi-quantify the constituent elements [15], [16]. Emission was recorded over approximately 200–900 nm, and the system provided a semi-quantitative estimate of the determined light and minor elements together with a presumed material classification. The same instrument provided an optical three-dimensional reconstruction of the slag surface in a height/colour mode, from which the surface relief was measured against a calibrated height scale spanning 0–44.86 µm.

Results and Discussion

Microstructure and composition of the Hadfield steel.

The secondary-electron micrograph of the polished steel (Fig. 1) shows a continuous matrix decorated by a dense network of fine, elongated dark features arranged in an intersecting, criss-cross pattern. This morphology is consistent with carbides and non-metallic particles distributed through a cast austenitic matrix, the characteristic structure of as-cast Hadfield steel [3], [5]. The EDS spectrum of the area (Fig. 2) is dominated by iron, identified by its intense Kα lines at around 6.4 keV and Lα lines at around 0.7 keV, with a clear contribution from manganese and minor peaks for carbon, oxygen, chromium and silicon. Weak signals of copper and chlorine were also detected; given that copper (Lα near 0.93 keV) and chlorine generally originate from embedding media and polishing, and considering the standardised, non-calibrated nature of the EDS quantification, these signals were regarded as probable artefacts related to the preparation rather than as actual

constituents of the alloy [17]. The iron-rich signature containing manganese is fully consistent with a high-manganese austenitic steel. [1].

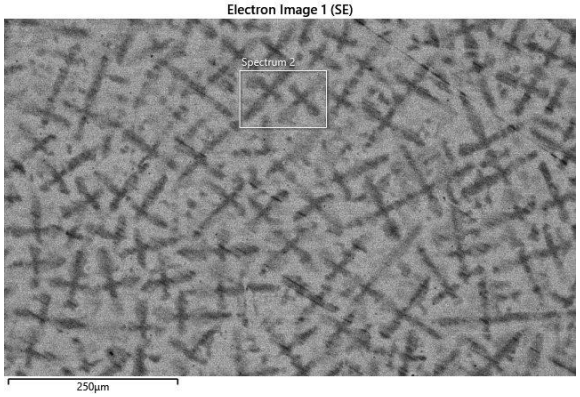

Fig. 1. Secondary-electron (SE) micrograph of the polished Hadfield steel, showing the austenitic matrix decorated by an intersecting network of fine carbide/inclusion features.

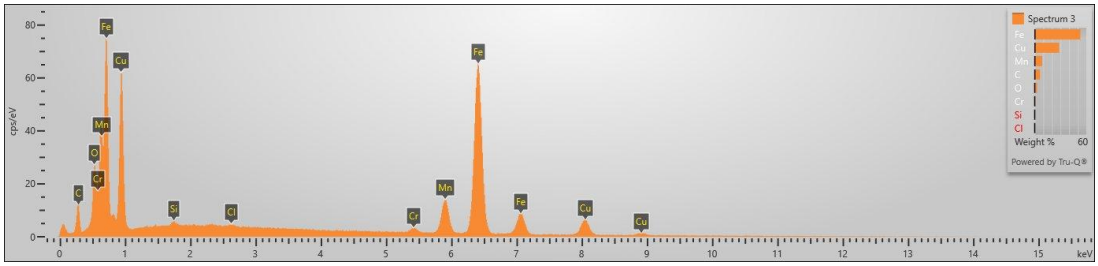

Fig. 2. EDS area spectrum of the Hadfield steel (iron-dominant, with manganese and minor C, O, Cr and Si; trace Cu and Cl attributed to sample preparation). Line scan and elemental mapping: a (Fe,Mn)-oxide–silicate inclusion.

In order to analyse variations in composition within the microstructure, an EDS profile was taken over a length of approximately 62 µm (Fig. 3). Along most of the profile, the elemental concentrations remained broadly constant, but a marked variation was observed in the central region, between approximately 20 and 35 µm. There, the oxygen signal rose sharply to a maximum of about 2600 counts per second and the carbon signal showed a smaller concurrent rise, while the iron and manganese signals dipped simultaneously over the same interval. The elemental maps (Fig. 4) confirm this behaviour spatially: oxygen is concentrated within a discrete, cross-shaped domain rather than being uniformly distributed, whereas iron, manganese and copper are spread broadly across the field of view.

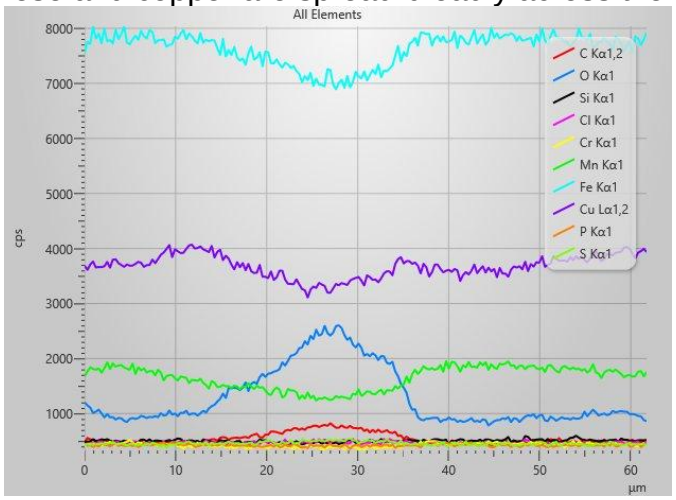

Fig. 3. EDS line-scan profiles across the steel microstructure. Oxygen (and, to a lesser extent, carbon) peaks in the central region while iron and manganese are simultaneously depleted, indicating a non-metallic oxide inclusion.

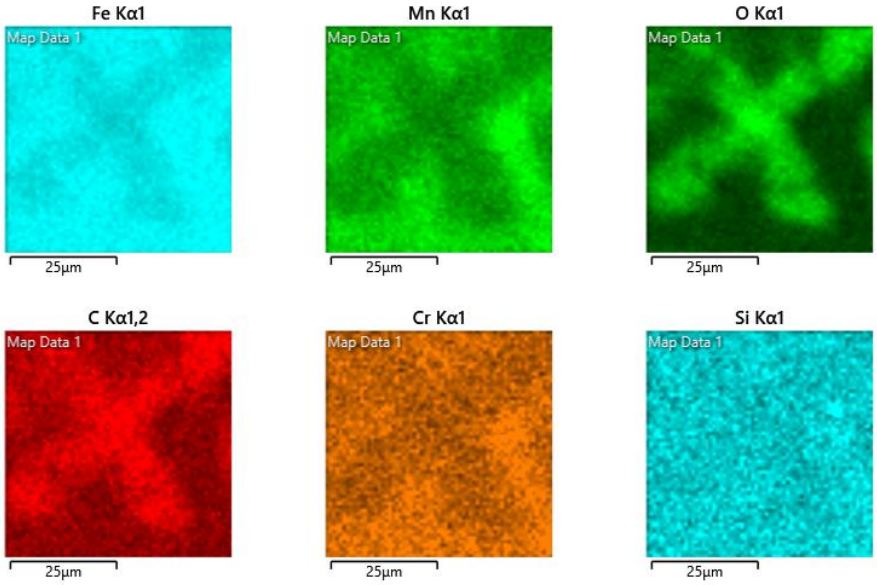

Fig. 4. SEM–EDS elemental maps of the steel (Fe, Mn, O, C, Cr, Si). Oxygen is concentrated within a distinct cross-shaped domain, in contrast to the broadly distributed matrix elements.

The spatial anticorrelation of oxygen (enriched) with the matrix elements, iron and manganese (depleted), together with a slight carbon enrichment, is the classic signature of a non-metallic oxide inclusion: an oxygen-rich particle embedded in the metallic matrix and chemically distinct from it [17]. The main deoxidising elements in this steel are manganese and silicon. The inclusion is best understood as a (Fe,Mn)-oxide / manganese-silicate phase, a deoxidation product formed as these elements removed dissolved oxygen. Direct evidence for this interpretation can be found in the Fe–Mn–O system, where higher manganese and oxygen contents form a non-metallic liquid oxide phase (similar to slag) within the steel [17]. The inclusion observed here is the solidified residue, on a micrometre scale, of this same oxide system, trapped within the metal.

Surface topography investigation togather with LIBS chemistry of the slag. The 3D optical reconstruction of the surface of the slag (Fig. 5) displays an irregular and rough topography with random raised nodular features above the surface.

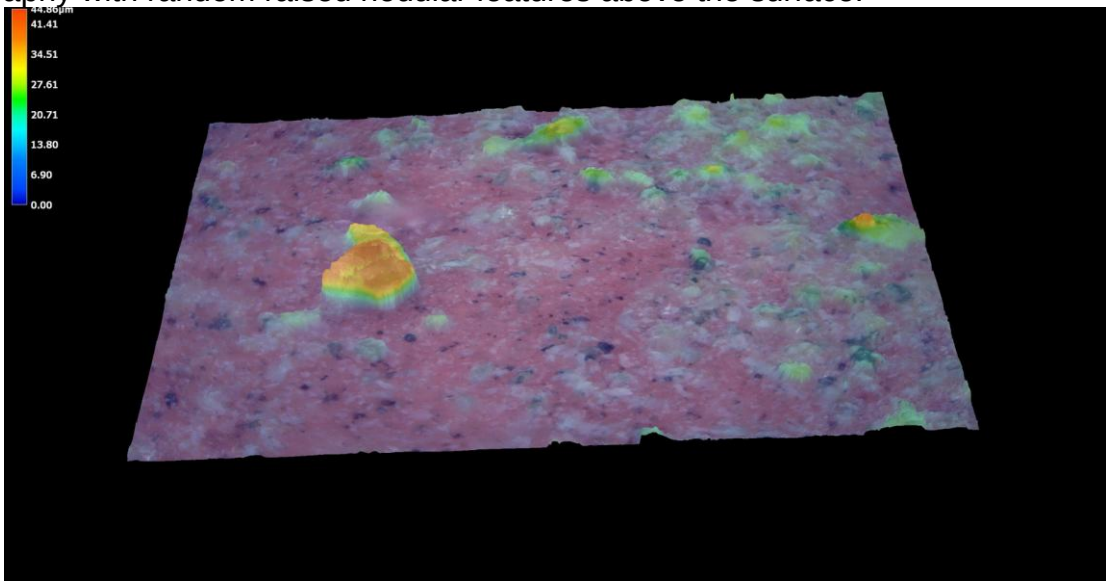

Fig. 5. Three-dimensional optical profilometry reconstruction of the steelmaking-slag surface (height/colour mode). The colour scale indicates surface height; the maximum measured relief is 44.86 µm.

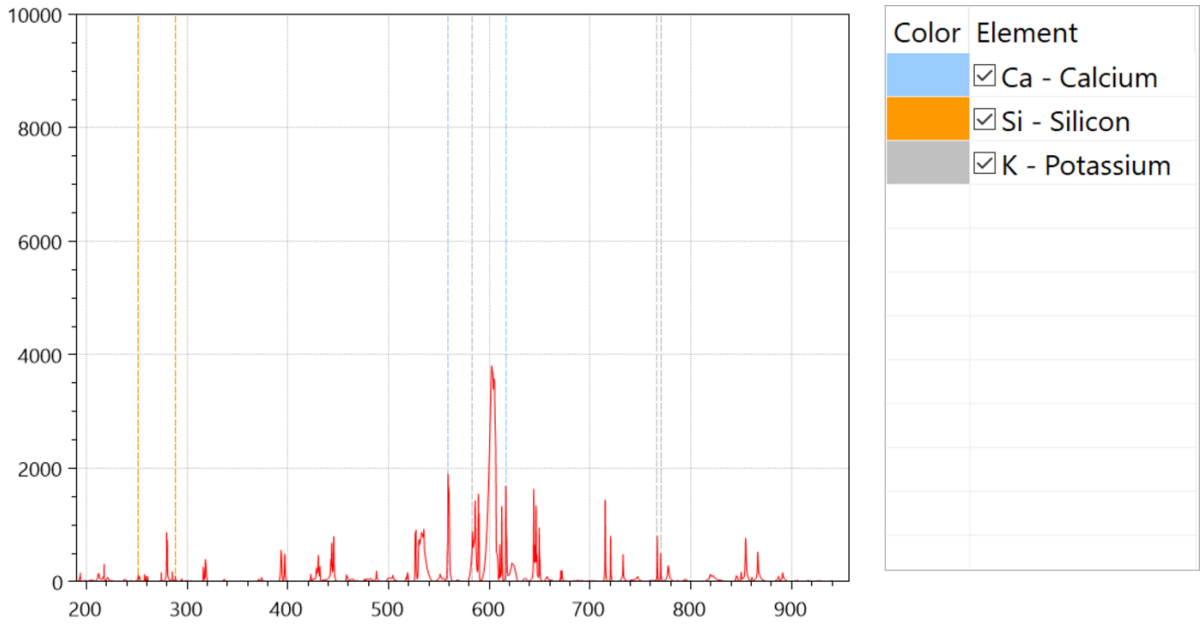

Fig. 6. LIBS emission spectrum of the slag (≈200–900 nm). Marker lines indicate the detected calcium (blue), silicon (orange) and potassium (grey) emission positions; calcium dominates the spectrum.

The maximum measured relief was 44.86 µm, with a pronounced mound rising to the top of the height scale. An uneven and nodular surface with significant local relief is characteristic of electric arc furnace slag that has solidified at differing rates [8]. The LIBS emission spectrum of the same material (Fig. 6) spans approximately 200–900 nm and is dominated by calcium emission lines, most notably near 616 nm and 559 nm, accompanied by weak silicon lines near 251.6 and 288.2 nm and by potassium lines, including the characteristic resonance doublet near 766.5 and 769.9 nm together with a line near 583 nm. On this basis the system classified the material as a calcium compound. The semi-quantitative contents determined among the measured light elements were 0.729 wt% calcium, 0.195 wt% silicon and 0.076 wt% potassium (Table 1).

Table 1.

LIBS semi-quantitative results for the slag and the principal detected emission lines.

Element	Principal emission lines (nm)	Content (wt%)
Calcium (Ca)	≈ 559, 616	0.729
Silicon (Si)	≈ 251.6, 288.2	0.195
Potassium (K)	≈ 583, 766.5, 769.9	0.076

Note: values are semi-quantitative and refer only to the determined light/minor elements; the oxide matrix, Fe and C are not quantified by this measurement.

The analysis, which covers only a selected set of light and trace elements and does not quantify the full oxide matrix or the iron and carbon contents, should be interpreted as a relative indicator of the elements determined rather than as a comprehensive chemical analysis; LIBS without a standard is, by its very nature, semi-quantitative and matrix-sensitive [15], [16]. Nevertheless, the calcium-silicon (-potassium) signature unambiguously classifies the slag within the CaO-SiO_2 (calcium silicate) system characteristic of steelworks slags, potassium being a minor alkaline constituent [8], [9].

Similarities and correlations between the steel and its slag

Combining the two datasets reveals a coherent and complementary picture of the steel-slag system. Firstly, the analyses show a clear distribution of elements between the two products: iron and manganese, which are alloy and matrix elements, are predominant

in the steel, whilst calcium, silicon, oxygen and potassium, which form oxides and fluxes, are predominant in the slag. Read jointly, the SEM–EDS and LIBS results effectively reconstruct how the elements distributed themselves between metal and slag during electric-arc-furnace refining (Table 2).

Table 2.

Complementary distribution of elements between the steel (SEM–EDS) and its slag (LIBS).

Element	Steel (SEM–EDS)	Slag (LIBS)
Fe	Matrix (dominant)	Not quantified
Mn	Principal alloying element	Minor (as MnO)
O	Inclusion-forming (local)	Structural (oxides)
Si	Minor (matrix/inclusion)	Major slag former
Ca	Not detected	Dominant
C	Matrix + inclusion	Not quantified
K	Not detected	Minor (alkali)

Second, silicon and oxygen act as bridging elements common to both products. Silicon appears as a minor constituent of the steel matrix and its inclusions and simultaneously as a major slag former, while oxygen is both the inclusion-forming element inside the steel and the structural element of the slag oxides. These shared elements are the chemical link between the metal and its slag.

Thirdly, and most importantly, the iron and manganese silicate oxide present in the steel belongs to the group of silicate oxides that make up the main slag. This means that the inclusion is in fact a chemical product of the slag trapped on a small scale within the metal. It is a product formed within the metal itself during its manufacture, and not an element originating from outside. This helps us to understand the link between the small-scale phenomena observed under a scanning electron microscope and the large-scale phenomena observed using a laser spectrometer. Everything hinges on the interaction between the metal and the oxides. In this process, manganese and silicon contribute to the removal of oxygen, and the oxides formed either rise back into the slag or remain trapped within the metal in the form of inclusions. Iron and manganese silicate oxide plays a role in this process.

Fourthly, manganese is a case in point. It is the element added to steel to impart the desired properties, such as those of Hadfield steel. However, some of the manganese always ends up in the slag. Some of the manganese is trapped in the inclusions in the form of manganese oxide. Controlling its distribution is crucial to ensure that the steel contains the required amount of manganese, i.e., between 11 and 14% by weight. Iron-manganese silicate oxide is also important in this process. It is also essential to consider the recovery of the manganese contained in the slag, as it is a valuable resource that must not be wasted. The manganese present in the slag is still manganese and can be reused; it is therefore necessary to find a way to recover it [1], [14].

Finally, the two techniques are genuinely complementary as characterisation tools. SEM–EDS provides spatially resolved morphology and micro-composition and is sensitive to light elements, but is subject to matrix effects and to the limitations of standardless, normalised quantification [19]; LIBS provides rapid, near-line, bulk multi-element analysis that also captures light elements, but is itself semi-quantitative and matrix-sensitive [15], [16]. The combined use of these methods enables the study of the material, from submicrometre-scale inclusions to the slag as a bulk material. From an application perspective, the significance lies in the fact that the oxide inclusions present in steel

constitute ‘discontinuities’ to which the toughness and purity of the material are linked. Determining the nature and location of these inclusions therefore enables process and quality control. It is also important to note that the slag composition is very rich in calcium and silicon, which allows for its reuse as cement and a construction material, as well as the recovery of small quantities of manganese [10], [11], [12], [13]. Of course, these observations must be qualified by the chemical heterogeneity of the slag, the possibility of preparation artefacts (copper and chlorine in EDS and potassium on the surface in LIBS), and by the semi-quantitative nature of EDS (lack of a standard) and LIBS (lack of calibration). These factors argue in favour of complementary methods of comprehensive analysis, such as X-ray fluorescence (XRF), inductively coupled plasma atomic emission spectrometry (ICP) or wavelength dispersive spectroscopy, when certified compositions are required.

Conclusion

A single pour of Hadfield steel and its steelworks slag were analysed using complementary techniques. SEM–EDS of the steel revealed an iron-rich austenitic matrix in which manganese is the principal alloying element, decorated by carbide/inclusion features; line scanning and elemental mapping located a discrete oxygen- and carbon-enriched, iron- and manganese-depleted region identified as a (Fe,Mn)-oxide–silicate non-metallic inclusion, i.e. a manganese-/silicon-driven deoxidation product. LIBS analysis and optical profilometry of the slag revealed a calcium-silicon (and potassium) silicate compound with an irregular, nodular surface and a maximum relief of 44.86 µm.

The main finding is that micro-inclusions in steel and bulk slag share the same oxide-silicate chemistry: the inclusions are, in fact, micrometre-scale slag trapped within the metal. This links descriptions at the micrometre and macroscopic scales through a single deoxidation chemistry and demonstrates the value of combining spatial-resolution scanning electron microscopy coupled with energy-dispersive X-ray spectroscopy (SEM-EDS) with spatial resolution and rapid bulk laser-induced breakdown spectroscopy (LIBS) to characterise the steel-slag system at different scales. The results confirm the purity of the steel and the control of inclusions, the assessment of the potential for manganese recovery, and the reuse of calcium-rich slag in cement and construction. Future work should include quantitative cross-validation by X-ray fluorescence (XRF), inductively coupled plasma atomic emission spectrometry (ICP-AES) or wavelength dispersive spectroscopy (WDS), the use of LIBS with or without calibration for comprehensive quantification of oxides, and the application of automated statistical analysis of inclusions via SEM-EDS to extend these observations, made on a single sample, to a representative population.

References

[1] R. Jacob, S. Raman Sankaranarayanan, and S. P. Kumaresh Babu, “Recent advancements in manganese steels – A review,” Mater. Today Proc., vol. 27, pp. 2852–2858, 2020, doi: 10.1016/j.matpr.2020.01.296.

[2] S. A. Torabi, K. Amini, and M. Naseri, “Investigating the effect of manganese content on the properties of high-manganese austenitic steels,” 2017.

[3] D. Gorlenko, K. Vdovin, and N. Feoktistov, “Mechanisms of cast structure and stressed state formation in Hadfield steel,” China Foundry, vol. 13, no. 6, pp. 433–442, 2016, doi: 10.1007/s41230-016-6105-8.

[4] D. V. Lychagin, A. V. Filippov, O. S. Novitskaia, Y. I. Chumlyakov, E. A. Kolubaev, and O. V. Sizova, “Friction-induced slip band relief of Hadfield steel single crystal

oriented for multiple slip deformation," Wear, vol. 374–375, pp. 5–14, 2017, doi: 10.1016/j.wear.2016.12.028.

[5] M. Sabzi, S. M. Far, and S. M. Dezfuli, "Effect of melting temperature on microstructural evolutions, behavior and corrosion morphology of Hadfield austenitic manganese steel in the casting process," Int. J. Miner. Metall. Mater., vol. 25, no. 12, pp. 1431–1438, 2018, doi: 10.1007/s12613-018-1697-1.

[6] G. Park, S. Jeong, and C. Lee, "Fusion weldabilities of advanced high-manganese steels: a review," Met. Mater. Int., vol. 27, no. 7, pp. 2046–2058, 2021, doi: 10.1007/s12540-020-00706-9.

[7] H. Yi, G. Xu, H. Cheng, J. Wang, Y. Wan, and H. Chen, "An overview of utilization of steel slag," Procedia Environ. Sci., vol. 16, pp. 791–801, 2012, doi: 10.1016/j.proenv.2012.10.108.

[8] I. Z. Yildirim and M. Prezzi, "Chemical, mineralogical, and morphological properties of steel slag," Adv. Civ. Eng., vol. 2011, pp. 1–13, 2011, doi: 10.1155/2011/463638.

[9] C. Navarro, M. Díaz, and M. A. Villa-García, "Physico-chemical characterization of steel slag. Study of its behavior under simulated environmental conditions," Environ. Sci. Technol., vol. 44, no. 14, pp. 5383–5388, 2010, doi: 10.1021/es100690b.

[10] R. Roychand, B. K. Pramanik, G. Zhang, and S. Setunge, "Recycling steel slag from municipal wastewater treatment plants into concrete applications – a step towards circular economy," Resour. Conserv. Recycl., vol. 152, p. 104533, 2020, doi: 10.1016/j.resconrec.2019.104533.

[11] Y. N. Dhoble and S. Ahmed, "Review on the innovative uses of steel slag for waste minimization," J. Mater. Cycles Waste Manag., vol. 20, no. 3, pp. 1373–1382, 2018, doi: 10.1007/s10163-018-0711-z.

[12] J. O'Connor et al., "Production, characterisation, utilisation, and beneficial soil application of steel slag: a review," J. Hazard. Mater., vol. 419, p. 126478, 2021, doi: 10.1016/j.jhazmat.2021.126478.

[13] W. Gao et al., "Comprehensive utilization of steel slag: a review," Powder Technol., vol. 422, p. 118449, 2023, doi: 10.1016/j.powtec.2023.118449.

[14] M. S. M. Zahar, F. M. Kusin, and S. N. Muhammad, "Adsorption of manganese in aqueous solution by steel slag," Procedia Environ. Sci., vol. 30, pp. 145–150, 2015, doi: 10.1016/j.proenv.2015.10.026.

[15] V. Sturm, R. Fleige, M. de Kanter, R. Leitner, K. Pilz, D. Fischer, G. Hubmer, and R. Noll, "Laser-induced breakdown spectroscopy for 24/7 automatic liquid slag analysis at a steel works," Anal. Chem., vol. 86, no. 19, 2014, doi: 10.1021/ac5022425.

[16] A. K. Myakalwar, C. Sandoval, M. Velásquez, D. Sbarbaro, B. Sepúlveda, and J. Yáñez, "LIBS as a spectral sensor for monitoring metallic molten phase in metallurgical applications – a review," Minerals, vol. 11, no. 10, p. 1073, 2021, doi: 10.3390/min11101073.

[17] Sayfidinov O, Tan S, Mardonov B, Sayfidinova M, Kumar B. Multi-Scale Characterization of Industrial Steel Slags Using XRF and SEM–EDS Phase Mapping. Crystals. 2026 Apr 7;16(4):246. https://doi.org/10.3390/cryst16040246.

[18] Sayfidinova, Makhliyo, Bakhtiyor Mardonov, and Okhunjon Sayfidinov. "Chemical analysis of steel slag by laser-induced decomposition spectroscopy analysis." In Third International Conference on Optics, Materials Science, and Computing in Condensed-Matter Physics (OMCCP-2025), vol. 14126, pp. 36-39. SPIE, 2026. https://doi.org/10.1117/12.3110743.

[19] S. K. Michelic, "Study on the possible error due to matrix interaction in automated SEM/EDS analysis of nonmetallic inclusions in steel by thermodynamics, kinetics and electrolytic extraction," Metals, vol. 10, no. 7, p. 860, 2020, doi: 10.3390/met10070860.